Effect of Molecular Relaxation of Acrylic Elastomers on Impact Toughening of Polybutylene Terephthlate

Nafih Mekhilef, Sheng Hong, Benjamin Davis

Arkema Inc., Research and Development Center, King of Prussia, Pennsylvania 19406

Received 15 December 2006; accepted 16 May 2007
DOI 10.1002/app.26955
Published online 2 August 2007 in Wiley InterScience (www.interscience.wiley.com).

ABSTRACT: In this study, we examined the performance of two core-shell acrylic-based impact modifiers (AIM) prepared by emulsion polymerization. The rubber core was prepared from ethyl hexyl acrylate (EHA) and *n*-octyl acrylate (*n*-OA). In such as process, the particle size and particle-size distribution of the modifiers were precisely controlled, so that performance differences observed in polybutylene terephthlate (PBT), used as matrix resin, could only be interpreted in terms of the nature of the elastomeric component of the modifiers. When isolated, the rubber core of the modifiers showed identical glass transition temperatures (T_g) by differential scanning calorimetry (DSC) and dynamic mechanical analysis (DMA) despite the fact that they were made from two different acrylic monomers. Temperature-frequency superposition principle inferred from the classical WLF equation showed that the rubber components exhibit the same T_g at all frequencies including at the time scale at which mechanical impact typically occurs. However, significant differences in low temperature impact performance measured at $-30^{\circ}C$ using notched Izod impact test according to ASTM D 256 were obtained even though their rubber components had identical T_g. Such differences were attributed to the dynamic relaxation behavior of the rubber components and identified as inherent properties of the elastomers due to the structure of the monomers' repeat units. J Appl Polym Sci 106: 2831–2839, 2007

Key words: molecular relaxation; viscoelastic behavior; toughening; PBT; acrylic elastomers

INTRODUCTION

Many thermoplastic resins are inherently brittle solids, especially at low temperatures and/or high strain rates, which limits their applications and use. To overcome their brittle behavior and expand their window of applications and life span, blending with other polymers and toughening modifiers has become a common practice in industry as indispensable part of plastics formulation. Throughout the years, the topic of polymer modification and especially toughening has attracted widespread attention both academically and industrially.[1–6]

Among all the common approaches to improve the toughness of polymers, modification via the addition of rubbers and/or elastomers forming a discrete phase in a given matrix resin is still the most effective mean of enhancing toughness. Today, commercial impact modifiers can be largely categorized into two groups: (1) linear polymers and (2) core shell particles. In the first case, a linear elastomer is typically blended with the matrix polymer in the molten state. The rubber domain size is controlled by the processing conditions (screw design, temperature, and shear), the rheology of the individual components (viscosity ratio and elasticity ratio), and the miscibility (interfacial tension and interaction parameter) between the modifier and matrix polymer.[7–9] The domain sizes are typically on the order of few microns and their distribution is generally of high polydispersity when the rubber phase is not crosslinked. In most cases, there is no crosslinking in the rubber domain. Nylon toughened by maleated EPDM is a typical example of this approach.[10] On the other hand, for core shell particles made from emulsion polymerization, the core is typically a crosslinked elastomer, which provides toughening properties, whereas the shell is typically a thermoplastic, which provides compatibility with the matrix and ease of handling of the product.[11] In this case, the particle-size distribution obtained is more uniform while a small particle size can be achieved. Typically, the domain size is in the order of few hundreds of nanometers, which would only affect impact strength while the rheology remains identical as the matrix.

Cavitation has been recognized as the key phenomenon responsible for an enhanced toughness of rubber-modified polymers.[12] It generally occurs by tearing and generating voids within the soft elastomeric phase or by debonding at the phase boundary when the stored volumetric strain energy within the

Correspondence to: N. Mekhilef (nafih.mekhilef@arkema.com).

elastomer phase exceeds a critical value. A quantitative description of such process was proposed by Lazzeri and Bucknall.[2,3] The energy density stored per particle after void formation is given by

$$\frac{U}{V_r} = \frac{K_r}{2}\left(\Delta_V - \frac{r^3}{R^3}\right)^2 + \frac{3\Gamma}{R}\left(\frac{r}{R}\right)^2 + \frac{3G_r F(\lambda_f)}{2}\left(\frac{r}{R}\right)^3 \quad (1)$$

where Γ is the surface energy of the rubber, G_r and K_r are the shear and bulk modulus, respectively, r and R are the radius for the void and the particle, and $F(\lambda_f)$ is a function of the elongation at break for the rubber phase. The first two terms are related to the energy required for the generation of the void, and the last term is related to the shear strain energy required to stretch the rubber and allowed it to expand. Both particle size and the modulus of the rubber have been shown to be important parameters affecting toughness.[12–14] The significance of particle size (R) has been established not only from a cavitation viewpoint as indicated by the equation above but also from the concept of critical interparticle distance, especially for semicrystalline polymers.[5,15] As for the properties of the rubber, it has been shown that the rubber with lower shear modulus could provide better toughness enhancement.[12–14] However, it is sometimes difficult to deconvolute the effect of particle size from the inherent properties of the rubber phase. This is especially true for linear polymers where the domain sizes are strongly influenced by processing conditions, and hence the viscosity ratio between the matrix and the modifier.

Emulsion polymerization allows the preparation of elastomeric particles with well-defined morphology and polydispersity with diameters ranging from 60 to 600 nm.[16] Unlike linear polymer modifiers where the domain size is strongly influenced by the processing conditions, the domain/particle size of core-shell modifiers is predetermined by the synthesis procedure and is relatively insensitive to processing as long as adequate shear is provided to disperse the modifier to its primary particles. Consequently, core-shell modifiers allow one to decouple the effect of particle size and study the specific influence of rubber property on impact toughening.

In this study, we compared the toughening ability of two types of core shell impact modifiers made from two very similar acrylic elastomers: poly (*n*-octyl acrylate) and poly(2-ethylhexyl acrylate) (monomer structure shown in Scheme 1) as toughening agents for poly(butylene terephthlate) (PBT). Both modifiers were prepared using the same emulsion polymerization recipe, and they have essentially identical particle size and morphology. The core consists of a partially crosslinked acrylic rubber, and the shell consists of poly(methylmethacrylate) containing small amount of functional comonomer to enhance the miscibility of the particle with PBT.

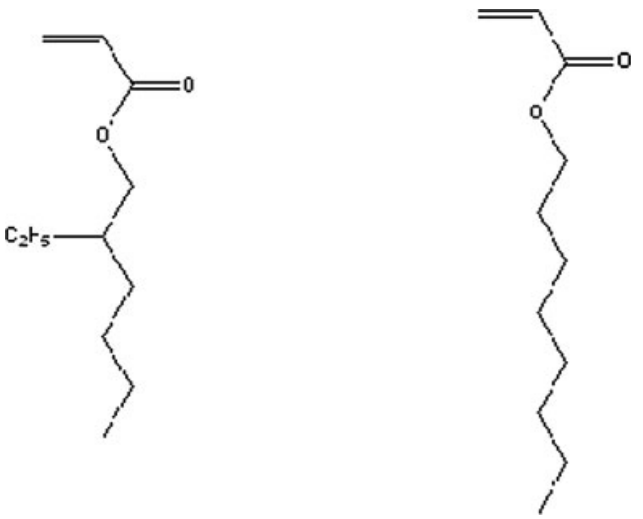

Scheme 1 Molecular structure of 2-ethyhexyl acrylate and *n*-octyl acrylate.

EXPERIMENTAL

Materials

All materials used in this work are either products of Arkema or chemical reagents obtained from Aldrich. The PBT used in this study is Celanese® 1600A extrusion grade with a density of 1.31 g/cc and a Rockwell M hardness of 72.

Synthesis

The core-shell modifiers were prepared by conventional semicontinuous emulsion polymerization method. The particle size of the modifier is controlled via the so-called grow-out ratio. Seed latex of poly(acrylate) was first prepared. A mixture of acrylic monomer (2-EHA or *n*-OA) and a small amount of multifunctional crosslinker monomer were then fed into the reaction kettle to grow the seed to the desired size. Afterward, MMA monomer was fed into the reactor to form the shell. The sizes of the particle were evaluated by both CHDF and dynamic light scattering and found to be monodispersed with polydispersity below 1.2. The particle diameters of all modifiers studied were carefully controlled and were within ±20 nm. The modifier powders were then isolated via freeze-thaw method. The powder sizes were in the range of few hundreds of microns.

Compounding and injection molding

Celanese 1600A PBT resin was used in this study as the matrix. The resin was dried at 60°C under vacuum for 6 h prior to use. Compounding was performed using a Leistriz® 18 mm twin-screw extruder. The screw assembly was designed for medium mixing and to ensure proper dispersion of the particles. The temperature was set to 235–255°C at the die. The compound was extruded and pelletized using an under water pelletizer and dried overnight under vacuum. The compounded pellets were then injection molded into ASTM Izod bars using Arbug® 50 injection-molding machine at 260°C.

Izod impact test

The Izod bars were notched according to ASTM D256 and aged in a constant relative humidity room (50% RH) for 40 h before testing. The Izod impact tests were conducted according to the specification reported in ASTM D256.

Thermal analysis

Differential scanning calorimetry was conducted using a TA Instruments DSC model 2920. The second heating obtained at a rate of 20°C/min was used for glass transition temperature determination.

Dynamic mechanical analysis

A Rheometric Scientific RDA III strain rheometer was used to conduct Dynamic Temperature Ramp tests using a torsion rectangular geometry with approximate sample dimensions of $2 \times [1/2] \times 1/16$ in^3. Testing was performed at a heating rate of 5°C/min, and a strain ranging from 0.03% to 0.5% at 1 Hz. All testing was conducted under forced convection nitrogen atmosphere between −150°C and 180°C.

The dynamic mechanical properties were measured on the real modifier synthesized by emulsion polymerization. Hence, the results obtained are direct indication of modifiers' properties.

Phase morphology

Atomic force microscopy (AFM) was used to examine the morphology of the blends. A cross section from the sample was cryo-microtomed using a RMC 990 rotary microtome with a CRT 900 cryogenic attachment. Both the sample and cutting knives (glass and diamond) were kept at a temperature of −100°C. AFM images were collected in Tapping Mode using a RTESP14 etched silicon probe, and both height and phase data were recorded. Additionally, scanning electron microscopy was used to examine the phase morphology. Samples were cryo-microtomed at an angle perpendicular to the fracture surface. Around 10 nm of Palladium was sputter coated onto the sample surface. SEM images were obtained using the In-Lens detector of a LEO 1530 field emission electron microscope.

Measurement of T_2 via ^{1}H NMR

Static ^{1}H Hahn spin echo measurements were performed using a Bruker DMX300 equipped with a 4 mm CPMAS probe. ^{1}H 90° and 180° pulses were set to 1.75 and 3.5 μs, respectively. Samples were dried in a vacuum oven and then packed into 4 mm rotors under dry nitrogen in a glove box.

RESULTS AND DISCUSSION

Low temperature impact properties

Summarized in Table I are four core-shell modifiers synthesized by emulsion polymerization. The elastomer components of samples A and B were made from *n*-octyl acrylate and 2-ethyl hexyl acrylate (EHA), respectively. Identical amount of multifunctional crosslinking agent was used in samples A and B and were higher than samples C and D.

Shown in Figure 1 are representative DSC second heat thermograms of samples C and D. With identical amount of crosslinking agent, poly(*n*-OA) exhibits slightly higher T_g and more pronounced hysteresis than poly(2-EHA). Curve integration revealed a T_g of −63°C for sample C while for sample D, the T_g was found to be −66°C. This difference is real but not considered meaningful, especially in terms of impact performance. The size of the hyster-

TABLE I
Summary of Different Core Shell Impact Modifiers Used in this Study

Sample ID	Core component	Crosslinker %	Core T_g by DSC (°C)	Shell component	Particle size	PDI
A	Poly(*n*-OA)	High	−61	PMMA	Identical (±20 nm)	<1.2
B	Poly(2-EHA)		−64			
C	Poly(*n*-OA)	Low	−63			
D	Poly(2-EHA)		−66			

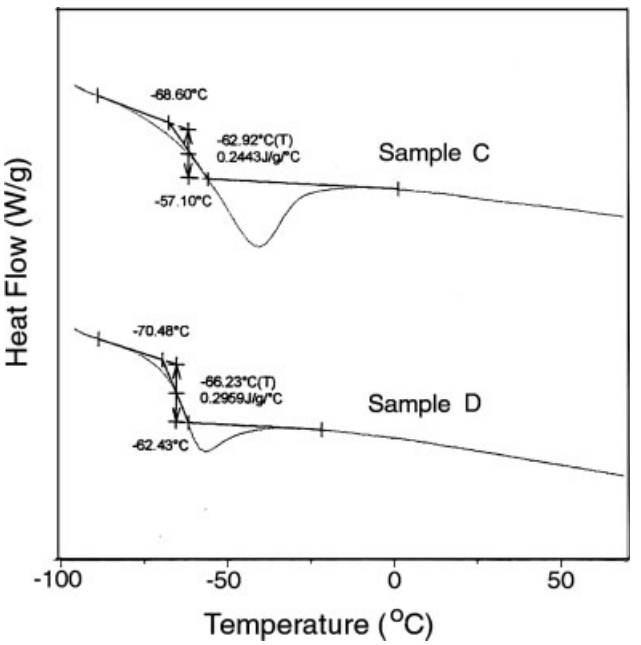

Figure 1 DSC thermograms of sample C and sample D.

esis peaks is a reflection of the testing conditions and can be altered by changing the heating and cooling rates. Samples with higher amount of crosslinker (A and B) showed slightly higher T_gs (A: -61°C and B: -64°C) consistent with the predictions of rubber elasticity theory suggesting a higher a T_g for a higher crosslink density.

Figure 2 is an AFM micrograph showing dispersion of sample A in PBT at 25% loading. The small dark domains are primary particles of the core shell impact modifier. Near ideal dispersion similar to the morphology shown in Figure 2 was achieved for all samples studied. The impact properties of those blends were then evaluated according to ASTM D256 and summarized in Table II.

Figure 3 shows the SEM micrographs of sample D after being impact tested at -30°C (which has mostly ductile failure at -30°C). The specimen was microtomed at -150°C at an angle perpendicular to the fracture surface as depicted in the schematic. Except for sample B, all samples showed similar fractography at -30°C test temperature. The formation of defined dilatational bands and pronounced cavitation were observed for all samples exhibiting ductile behavior. These suggest that the governing toughening mechanism is by dilatational yielding facilitated by rubber cavitation. Sample B exhibits a brittle behavior at -30°C, and no cavitation bands are observed under SEM. Additionally, pronounced stress whitening was observed for all samples showing a ductile behavior.

As shown in Table II, samples with lower amount of crosslinking agents (C and D) always performed better in terms of impact strength. It shall be noted that due to the complexity involved with acrylate copolymerization, and although samples A and B (similarly C and D) have identical charges of crosslinking agents, the degree of crosslinking in the elastomer network between A and B could not be know *a priori* since the polymerization chemistry and kinetics of *n*-OA versus 2-EHA might be different. On the other hand, it is reasonable to conclude, in accordance with the DSC results, that sample A has higher crosslink density than samples C and B, and samples C and D have higher crosslink density than sample D. The observation that samples with lower crosslink density have better impact toughness can be explained by the cavitation model described in eq. (1). Since all modifiers have identical particle sizes, the radius of cavitation becomes extremely sensitive and is predominantly controlled by the degree of crosslinking. Any difference observed in impact data is related to the inherent property of the rubber component (crosslinking). The modifiers with the higher crosslink density (A and B) typically would exhibit higher shear modulus (this point will be discussed further) and hence more difficult to expand leading to higher resistance to cavitation and poorer impact properties. In contrast, the samples with lower crosslink density would show a lower shear modulus and would be more prone to expansion thus leading to cavitation easily. Therefore, the relationship between the crosslinking density, the modulus, and the cavitation is well established in terms of its impact on toughening the matrix.

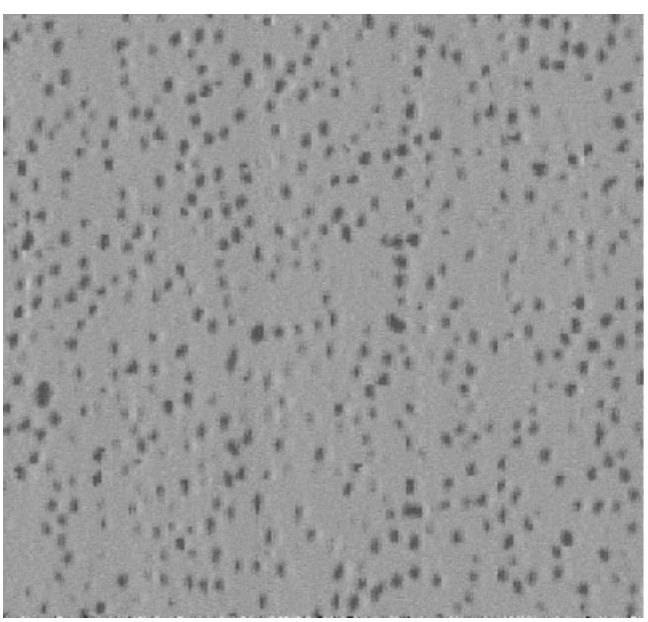

Figure 2 AFM micrograph of PBT blended with 25% modifier A (The scale bar is not shown due to proprietary information. The size of the particle is in the range of 60–600 nm).

TABLE II
Summary of Izod Impact Properties of PBT Toughened by Core Shell Modifiers at Different Temperatures

	Impact properties (ft-lb/in)			
Sample ID	25°C impact	−20°C impact	−30°C impact	−40°C impact
A	100%D (15.5)	–	86%D (15.8/4.2)	–
B	100%D (13.5)	57%D (13.7/3.4)	0%D (3.1)	–
C	100%D (15.9)	–	100%D (15.5)	57%D (11.7/5.4)
D	100%D (12.2)	–	86%D (15.4/3.8)	–

Interestingly, at both high and low crosslinker concentration, the modifiers made with poly(*n*-octyl acrylate) always performed better than modifiers made with poly(2-ethylhexyl acrylate) even though DSC results suggest identical T_g for both elastomers. There is no apparent explanation from the results thus for nine crosslink density and glass transition temperature.

Dynamic relaxation properties

The T_gs obtained from DSC thermograms were obtained under quiescent conditions (frequency $\omega \sim 0$ or infinite time). However, impact testing, especially Izod impact testing typically occurs at a time scale in the order of milliseconds and corresponds to a high frequency phenomenon. Dynamic mechanical analysis at different frequencies was performed to better understand the elastic behavior of these materials at higher frequencies.

Core-shell modifier samples were compression molded into rectangular bars and evaluated by DMA under torsional mode at different frequencies. The tan δ responses of poly(*n*-OA) and poly(2-EHA) obtained from 0.3 to 50 Hz in shown in Figure 4(a,b). The glass transition of polymers follows the classical WLF equation. For which, a variant version can be expressed as

$$T_g' = T_g + \frac{C_1 \times \log \alpha_T}{C_2 - \log \alpha_T} \quad (2)$$

In this format, the shift factor α_T is the ratio of the test frequencies. Taking the results at 0.3 Hz as the reference frequency, the plot in Figure 5 was obtained. The peak temperature of tan δ was used as the parameter of interest in this plot. Within the frequency range studied, the WLF plot of poly(2-EHA) and poly(*n*-OA) coincided with each other, and there was no apparent sign of divergence suggesting that if extrapolated to higher frequencies, the peak T_g value of the two polymers should still be very similar. Curve fitting to the proposed WLF equation gave values of $C_1 = 60$ and $C_2 = 14$, in fair agreement with the well-established empirical values of $C_1 = 51.6$ and $C_2 = 17.44$. In addition, at every frequency, poly(2-EHA) actually showed a lower T_g (peak temperature, about 2°C) than poly(*n*-OA) consistent with the DSC results. Accordingly, the frequency dependence of T_g is not the main reason for the observed impact performance difference between the two elastomers.

On the other hand, Figure 4 also revealed a very interesting phenomenon. The breadth of the glass transition peak of poly(2-EHA) appears to be wider than that of poly(*n*-OA), and the difference becomes much more dramatic with increasing frequency. At high frequencies, the onset of tan δ transition for poly(2-EHA) was significantly higher than that of poly(*n*-OA).

Figure 6 is a plot of the full width half maximum (FWHM) as a function of frequency. This representation is common in spectroscopy and has been used by many to conduct quantitative analysis of spectroscopic data. The FWHM of poly(2-EHA) exhibits

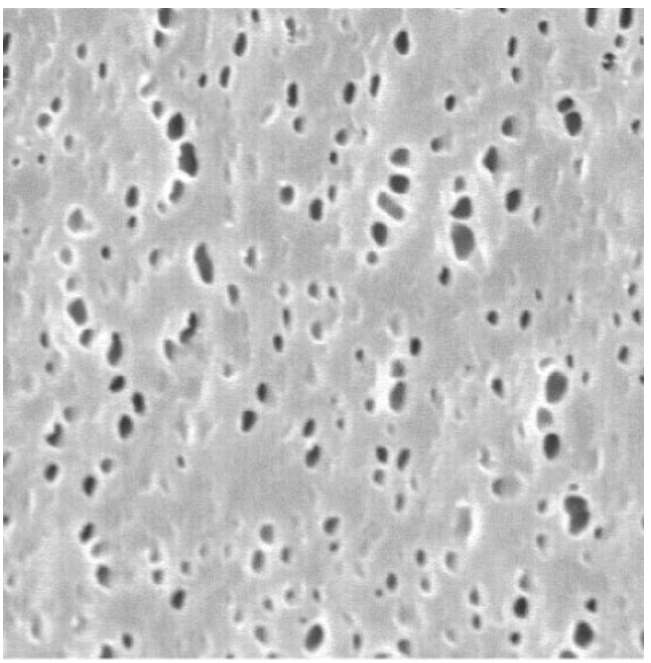

Figure 3 SEM of PBT toughened by core-shell modifier sample D. The sample was fracture under Izod test at −30°C. The micrograph was taken at regions just below the fracture surface.

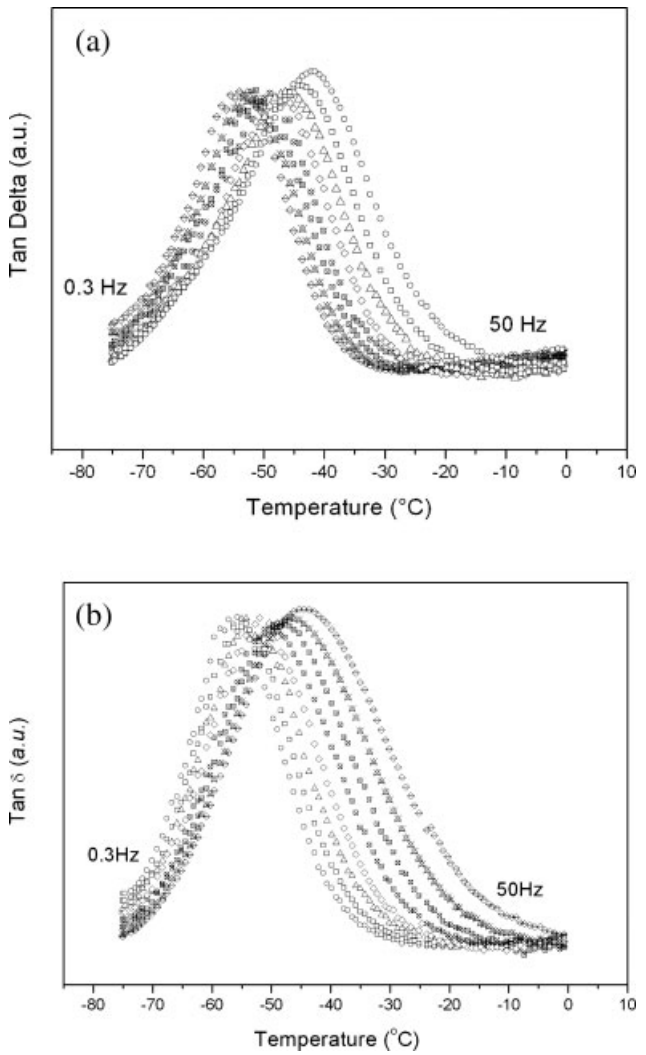

Figure 4 (a) Tan δ transition as a function of frequency (0.3, 0.6, 1.2, 2.4, 5.4, 11.2, 24.9, and 50 Hz) obtained in DMA under torsion mode. Response from poly(*n*-octyl acrylate) rubber core in sample A. (b) Tan δ transition as a function of frequency (0.3, 0.6, 1.2, 2.4, 5.4, 11.2, 24.9, and 50 Hz) obtained in DMA under torsion mode. Response from poly (2-ethylhexyl acrylate) rubber core from sample B.

much stronger frequency dependence with higher frequency giving higher value of FWHM. The FWHM of tan δ transition (specifically tan δ versus $1/T$) is an indication of both the activation energy of the molecular motions responsible and the breath of the transition. The activation energy of glass transition, which is governed by free volume effect, is not an invariant but rather temperature dependent. It is difficult to obtain definitive description of the FWHM of tan δ transition under isochronal conditions. However, the observation that the peak T_g of poly(*n*-OA) and poly(2-EHA) followed the WLF relationship yet their FWHM showed significantly different dependence, suggesting that there are fundamental differences in the viscoelastic relaxation mechanisms between the two modifiers.

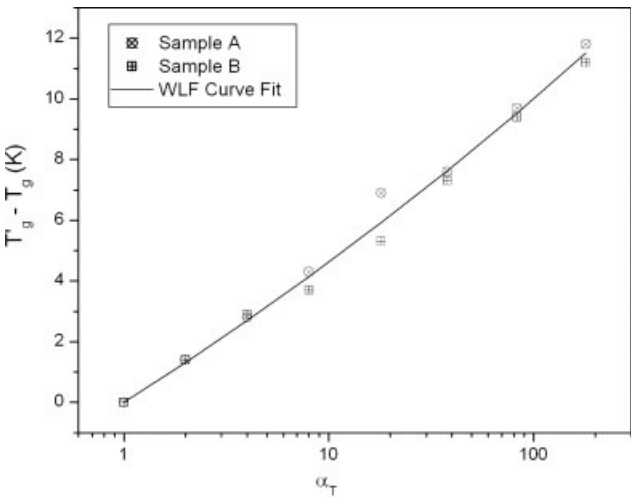

Figure 5 WLF plot of peak transition temperature as a function of the shift factor. Results at 0.3 Hz were used as reference state.

To further understand the ramification of this phenomenon and correlate it with the observed impact property differences, a separate series of dynamic relaxation experiments was carried out. The complex modulus of the rubber component of the core-shell modifier was measured as a function of temperature (Fig. 7) isochronally at 1 Hz. The experiments were conducted in such a way that only the rubber core response was evaluated, and the results were not influenced by the MMA-based shell or the morphology of the core shell particle.

The complex shear moduli (G^*) of the rubber cores of samples A through D as a function of temperature at 1 Hz are summarized in Figure 7. Because of the

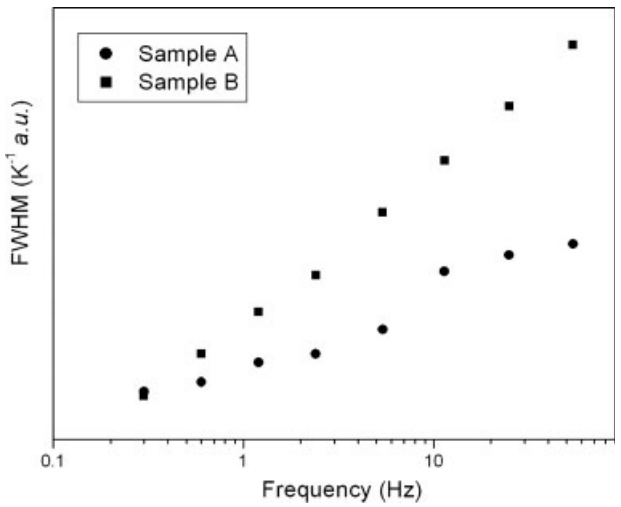

Figure 6 FWHM obtained from plots of tan δ versus $1/T$ plots (plots not shown) for samples A and B.

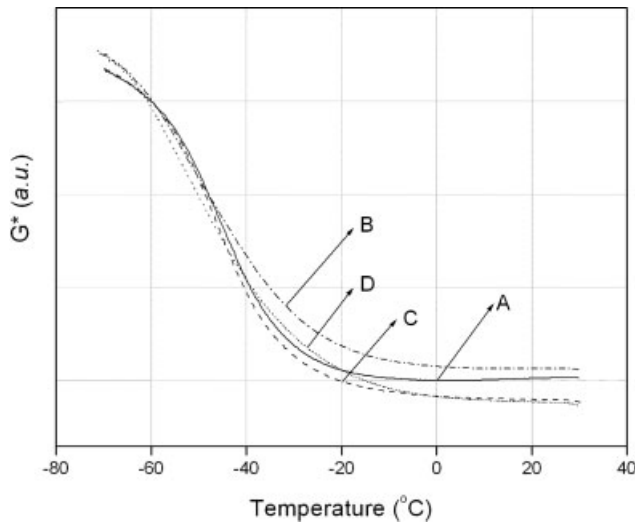

Figure 7 Dynamic shear modulus of samples A through D.

limitation of the current experimental setup, only responses at 1 Hz were measured in these sets of experiments. Hence, the results will be discussed in combination with the frequency study presented earlier.

First, all samples exhibit well-defined plateau modulus, which was a function of the amount of crosslinker used and the final crosslink density of the core. Second, the glassy modulus did not depend on the crosslinker level. Interestingly, the glassy modulus of poly(2-EHA) appeared to be much higher than that of poly(*n*-OA). This is primarily dominated by their chemical structure (linear versus branched). Comparing samples A and C with samples B and D, it was immediately apparent that the major difference between poly(*n*-OA) and poly (2-EHA) elastomers was their near T_g mechanical properties. The shear modulus of poly(2-EHA) elastomers started to show significant increase at a much higher temperature than poly(*n*-OA). The transition was much broader for poly(2-EHA) than it was for poly(*n*-OA). Accordingly, elastomers made from poly(2-EHA) would start to stiffen at a temperature higher than for poly(*n*-OA). Considering the previous results of FWHM at varying frequencies, it could be concluded that the differences between the two elastomers in the T_g region would be even more dramatic at higher frequencies.

From Table II, comparing samples A and D, using lower amount of crosslinking agents, sample D achieved similar performance as sample A. Sample C, which was based on poly(*n*-OA), still performed better and had about 10°C lower brittle-ductile transition temperature (BDDT). The low temperature impact properties of different modifiers followed qualitatively the shear modulus values measured from −20°C to −40°C (Fig. 7). Samples with lower shear modulus in this region gave better toughening properties. The results agreed well with the cavitation model and indicated that the resistance of rubber to expand was the main attribute differentiating one modifier from the other. When the test temperature was close to T_g, resistance to rubber cavitation was higher in the case of poly(2-EHA) at equal crosslink density. As a result, PBT toughened by poly(2-EHA)-based core-shell modifiers showed higher BDDT than those by poly(*n*-OA)-based modifiers.

An apparent question was whether the peculiar near-T_g behavior of poly(2-EHA) elastomer could be modified by chemistry such as further suppressing the crosslink reaction. Summarized in Table III was a series of poly(2-EHA)-based core-shell modifiers (samples E, F, and G). Dodecyl mercaptan (DDM) was used as a chain-transfer agent during the polymerization to further suppress and even eliminate crosslinking reactions. However, no further improvement was observed in the impact properties. The dependence of G^* for those elastomers as a function of temperature is shown in Figure 8. The addition of chain-transfer agent resulted in pronounced terminal behavior characteristic of noncrosslinked polymers. The G^* at room temperature became progressively lower due to the formation of more low molecular weight linear chains. However, there was no change in the near T_g mechanical properties. The shear moduli of the elastic component in the core-shell modifiers stayed constant at temperatures below −20°C. Consequently, no improvement in BDT was possible at low temperatures (results not shown). The G^* results were further substantiated by T_2 measure-

TABLE III
Summary of Different Core Shell Impact Modifiers Containing Chain Transfer Agents (DDM)

Sample ID	Core component	Crosslinker %	DDM %	Shell component	Particle size	PDI
E	Poly(2-EHA)	Low (identical to D)	Low	PMMA	Identical (±20 nm)	<1.2
F	Poly(2-EHA)		Medium			
G	Poly(2-EHA)		High			

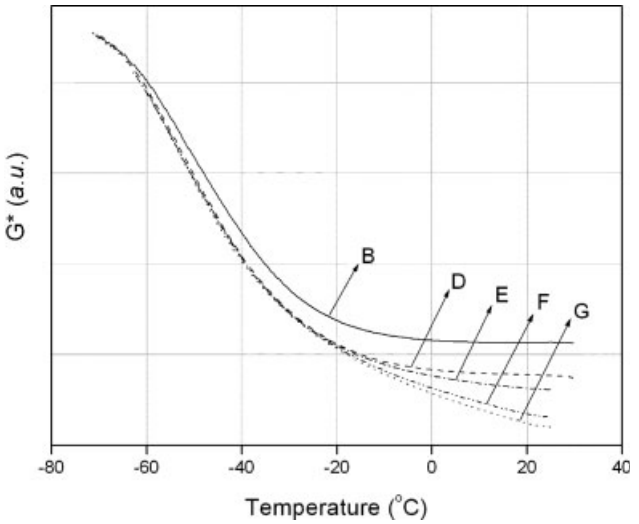

Figure 8 Dynamic shear modulus of samples E through G. Results of samples B and D were also included for comparison reasons.

ment by ^{1}H NMR, where the T_2 for samples D, E, F, and G showed significant differences at room temperature but basically identical at −30°C (Table IV). The above results indicated that the near T_g viscoelastic property differences between poly(*n*-OA) and poly(2-EHA) are not due to their chemistry but rather their inherent molecular structures.

It is hypothesized, based on data discussed, that the apparent glass transition of poly(2-EHA) observed in DMA, which appears to be much broader, most likely consists of more than one relaxation mode, possibly confronted with other relaxation modes such as a β-relaxation. α-Relaxation (T_g) follows WLF relationship whereas β-relaxation (secondary) follows Arrhenius relationship.[17,18] They have different temperature/frequency dependence that can lead to the observed FWHM broadening effect. Considering the structural difference between 2-EHA and *n*-OA molecules, the peculiar relaxation behavior of poly(2-EHA) is most possibly related to its branched side chain. This effect is manifested in toughening properties of core-shell modifiers.

Previous studies have observed similar confronted multiple viscoelastic mechanisms in methacrylic polymers.[19,20] However, no report on poly(2-EHA) was found in the literature. Currently, it is not entirely clear what the nature of the dynamic relaxation of poly(2-EHA) around T_g is, which is best to be investigated by dielectric spectroscopy and NMR. The main purpose of this report is to elucidate the significance of dynamic relaxation behavior of the toughening agent on impact properties where seemingly similar acrylic elastomers can have significant difference in their impact toughening capabilities. In addition, this study further indicates that shear modulus or crosslink density measured at room temperature and/or the peak T_g temperature are not sufficient to predict impact behavior at low temperatures due to the complexity involved in polymer relaxation dynamics.

TABLE IV
T_2 Relaxation Time Measured by ^{1}H NMR of Samples D, E, F, and G

Sample ID	DDM %	T_2 @ 25°C (μs)	T_2 @ −30°C (μs)
D	None	560	46
E	Low	710	44
F	Medium	770	47
G	High	810	47

CONCLUSIONS

In this article, the impact properties and toughening mechanisms of two acrylic elastomers with identical T_g and very similar monomer repeat units were studied. Core-shell modifiers made from poly(*n*-octyl acrylate) were found to provide better low temperature impact toughening properties to PBT than that of poly(2-EHA)-based impact modifier, although the apparent T_g for poly(*n*-OA) and poly(2-EHA) were found to be similar at all frequencies studied. The differences in impact properties were related to the stiffness of the rubber core through dynamic relaxation measurement and can be qualitatively explained by the cavitation theory derived by Lazzeri and Bucknall. Poly(2-EHA) elastomer differs from poly(*n*-OA) in their near-T_g mechanical properties, which manifested to affect the macroscopic impact test results at low temperatures. It is hypothesized that the peculiar near-T_g behavior of poly(2-EHA) is due to the confronted effect of α- and β-transitions, which may originate from the branched side chain of poly(2-EHA).

References

1. Bucknall, C. B. Toughened Plastics; Applied Science: London, 1977.
2. Lazzeri, A.; Bucknall, C. B. Polymer 1995, 36, 2895.
3. Lazzeri, A.; Bucknall, C. B. J Mater Sci 1993, 28, 6799.
4. Barham, B.; Fosser, K.; Voge, G.; Waldow, D.; Halasa, A. Macromolecules 2001, 34, 514.
5. Wu, S. Polym Int 1992, 29, 229.
6. Pearson, R. A.; Sue, H.-J.; Yee, A. F. Toughening of Plastics: Advances in Modeling and Experiments; Oxford University Press: Oxford, 2000.
7. Hobbs, S. Y.; Dekkers, M. E. Polymer 1988, 29, 1598.
8. Paul, D. R.; Barlow, J. W. J Macromol Sci Rev Macromol Chem Phys 1980, C18, 109.
9. Wu, S. Polym Eng Sci 1987, 27, 335.

10. Muratoglu, O. K.; Argon, A. S.; Cohen, R. E.; Weinberg, M. Polymer 1995, 36, 921.
11. Cruz-Ramos, C. A. In Polymer Blends, Vol. 2; Paul, D. R., Bucknall, C. B., Eds.; Wiley: New York, 2000; p 137.
12. Bucknall, C. B. In Polymer Blends, Vol. 2; Paul, D. R., Bucknall, C. B., Eds.; Wiley: New York, 1999; p 83.
13. Yee, A. F.; Pearson, R. A. J Mater Sci 1986, 21, 2562.
14. Ishai, O.; Cohen, L. J. Int J Mech Sci 1967, 9, 539.
15. Barkczak, Z.; Argon, A. S.; Cohen, R. E.; Weinberg, M. Polymer 1999, 40, 2347.
16. Lovell, P. A.; El-Aasser, M. S. Emulsion Polymerization and Emulsion Polymers; Wiley: Chichester, UK, 1997.
17. McCrum, N. G.; Read, B. E.; Williams, G. Anelastic and Dielectric Effects in Polymer Solids; Dover: New York, 1967.
18. Aklonis, J. J.; MacKnight, W. J. Introduction of Polymer Viscoelasticity, 3rd ed.; Wiley: New York, 2005.
19. Williams, G. Trans Faraday Soc 1966, 62, 2091.
20. Schroter, K.; Unger, R.; Reissig, S.; Garwe, F.; Kahle, S.; Beiner, M.; Donth, E. Macromolecules 1998, 31, 8966.